Valence bands and Fermi-surface topology of untwinned single-crystal $YBa_2Cu_3O_{6.9}$

J. G. Tobin
Lawrence Livermore National Laboratory, Livermore, California 94550

C. G. Olson and C. Gu
Ames Laboratory and Iowa State University, Ames, Iowa 50011

J. Z. Liu
Department of Physics, University of California, Davis, Davis, California 95615

F. R. Solal, M. J. Fluss, R. H. Howell, J. C. O'Brien, H. B. Radousky, and P. A. Sterne
Lawrence Livermore National Laboratory, Livermore, California 94550
(Received 1 July 1991)

The cleaved surfaces of untwinned, single-crystal $YBa_2Cu_3O_{6.9}$ have been probed with synchrotron-radiation photoemission, utilizing both high energy and angular resolution. Acute spectral structure was observed, both at the Fermi energy and at higher binding energies, particularly near the high-symmetry points of the two-dimensional Brillouin zone, $\bar{\Gamma}$, $\bar{X}$, $\bar{Y}$, and $\bar{S}$. Many band crossings of the Fermi energy were seen, with obvious and important differences between the bands near $\bar{X}$ and those near $\bar{Y}$. A large superconducting gap was not observed: The data are consistent with a gap of less than 10 meV. The assignment of bands and Fermi-level crossings to chain and plane states will be discussed, including comparisons to the predictions of theory, particularly local-density-approximation calculations.

I. INTRODUCTION

The utility of probing the electronic structure of high-temperature superconductors with photoemission has been well established.[1,2] Using high-resolution photoelectron spectroscopy, Olson *et al.*[2] were able directly to observe and measure the superconducting gap of cleaved $Bi_2Sr_2CaCu_2O_8$. The high angular ($\pm 1°$) and energy [full width at half maximum (FWHM) ≈ 32 meV] resolution were essential to following the bands and measuring the gap ($\Delta = 24$ meV) at various specific points in reciprocal space. Moreover, in the case of $Bi_2Sr_2CaCu_2O_8$, the photoemission results provided a fairly stringent test for theoretical models of the electronic structure: The experimental Fermi surface preserved not only the volume, but also the essence of the local-density-approximation-(LDA-) calculated Fermi surface.[2] The experimental bands near the Fermi level retained a strong resemblance to the LDA bands, but with a moderate mass enhancement. The success of this approach with $Bi_2Sr_2CaCu_2O_8$ provided encouragement for the application of photoelectron spectroscopy to the more complicated system $YBa_2Cu_3O_{7-\delta}$.

Previous photoemission investigations of $YBa_2Cu_3O_{7-\delta}$ underlined the need for the utilization of the best samples and highest resolution to provide the most stringent test of the various theoretical models. A lower-resolution (100-meV) study[3] of twinned $YBa_2Cu_3O_{6.9}$ illustrated the necessity of both higher-resolution and *untwinned* samples, so that the inequivalent $\bar{\Gamma}$-$\bar{X}$ and $\bar{\Gamma}$-$\bar{Y}$ directions can be probed separately. In twinned samples two almost orthogonal domains of the orthohormbic $YBa_2Cu_3O_{7-\delta}$ are present, such that macroscopically states along both $\bar{\Gamma}$-$\bar{X}$ and $\bar{\Gamma}$-$\bar{Y}$ are simultaneously sampled. This precludes the differentiation of chain [one-dimensional (1D)] from plane [two-dimensional (2D)] states. Nevertheless, this study showed the plausibility of LDA approach to modeling the Fermi surface of $YBa_2Cu_3O_{6.9}$. Other investigations[2,4] probed more deeply into the valence-band structure. The results of the study using cleaved, twinned samples[2] indicated that the valence bands may have a more dispersive character than $Bi_2Sr_2CaCu_2O_8$. An investigation using epitaxially grown $YBa_2Cu_3O_{7-x}$ films[4] has also been reported. In all of these studies, the absence of acute spectral structure, sharp and intense valence-band peaks, is marked. Some of this may be due to the complexity of the $YBa_2Cu_3O_{7-\delta}$ samples: the aforementioned twinning, surface instabilities,[5] possibly nonunique cleavage, and the disorder caused by variation of the oxygen stoichiometry. These complications also reflect challenges to theoretical modeling, ranging from differentiation of the impact of one- (chain) and two- (plane) dimensional bands to the quantification of the doping process. All of this bears out the need for an experimental investigation using the best samples and best resolution, if only to provide detailed criteria for the testing of sophisticated theoretical models such as correlated LDA (Ref. 6) and doped insulator approaches.

In this paper we report the results of a photoemission study of $YBa_2Cu_3O_{6.9}$ in which we have striven to utilize the highest-resolution and best samples. An example of our data is shown in Fig. 1. Note the acute spectral structure at both $B^F = 1$ and 0 eV (at the Fermi energy,

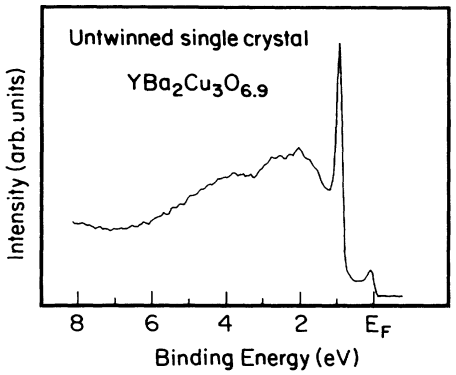

FIG. 1. Angle-resolved photoelectron spectrum of untwinned $YBa_2Cu_3O_{6.9}$ is shown here. The Brillouin zone near $\bar{X}$ was sampled, using $h\nu=24$ eV. Note the acute special structure at $B^F\cong 1$ and ≈ 0 eV. B^F is the binding energy with respect to the Fermi energy.

E_F). We have found that the combination of improved samples, in particular high-quality, untwinned, single crystals of $YBa_2Cu_3O_{6.9}$, and high-resolution angle-resolved photoemission can provide the type of detail that was previously missing in earlier investigations. This detailed information will thus permit us to map the valence bands and determine the Fermi crossings and superconducting gaps throughout the two-dimensional Brillouin zone: The emphasis will be on differentiating the nature and contributions of chain (1D) from plane (2D) states. To achieve this end, after the experimental section the paper is divided into three parts. In Sec. III A the valence-band structures will be considered with an emphasis upon the effects of detwinning and the sensitivity of spectral structure to sample quality in general. In particular, the family of states near $B^F=1$ eV will be described. These states exhibit sharp and intense peaks at $\bar{\Gamma}$, $\bar{S}$,$\bar{X}$, and $\bar{Y}$, with unique characteristics associated with each of those points in **k** space. This spectral structure not only provides a sensitive measure of sample quality, but also confirms the importance of the lattice and Brillouin zone in the conceptualization of the underlying basis of the electronic structure of this material. Section III B will discuss the Fermi surface and states near the Fermi surface. Band crossings have been mapped, with emphasis upon the inequivalent $\bar{\Gamma}$-$\bar{Y}$ and $\bar{\Gamma}$-$\bar{X}$ directions. Finally, Sec. III C contains a description of our superconducting gap measurements, throughout the Brillouin zone. Taken together, the results concerning the Fermi-surface topology of the cleaved surfaces of untwinned, single-crystal $YBa_2Cu_3O_{6-9}$ can be summarized as follows: (i) Crossings are seen throughout the two-dimensional Brillouin zone and are identified with plane- and chain-derived states; (ii) the electronic structures at $\bar{X}$ and $\bar{Y}$ are distinctly different; and (iii) the measured gap is zero or small throughout the two-dimensional Brillouin zone, for all of the observed bands, contrary to the preliminary reports of others.[7] This includes bands assigned as being of both chain and plane origin in LDA calculations. These and other experimental observations will be compared to the predictions of various theoretical models.

II. EXPERIMENT

All of the photoemission measurements were performed on the 1-GeV storage ring, Aladdin, at the University of Wisconsin Synchrotron Radiation Center (UWSRC), on the Iowa State University/Montana State University ERG/SEYA Beamline,[8] using an angle-resolved photoelectron spectrometer from Vacuum Science Workshop. The double-monochromator beamline incorporates both an extended-range grasshopper and a Seya-Namioka monochromator, for high- ($h\nu \gtrsim 30$ eV) and low- ($h\nu \lesssim 30$ eV) energy measurements, respectively. The electron and x-ray optics of the instrument have been optimized for utilization of the small $YBa_2Cu_3O_{3.9}$ samples ($\sim 1\times\sim 1$ mm^2, typically). The total-energy and electron-momentum resolutions are quite high: energy bandpasses of 30 meV or less are typical, and the electron angular acceptance is $\pm 1°$. The single crystals were grown and detwinned at University California-Davis.[9] Unless otherwise noted, the spectra and data are from untwinned, single crystals of $YBa_2Cu_3O_{6.9}$. The superconducting nature of the crystals was confirmed, prior to the photoemission experiments, by means of Meissner-effect measurements. A transition temperature near 93 K was observed, with transition widths of less than 3 K typical.[9] Samples were oriented, before and after cleaving, by the use of Laue-backscattering measurements. The sample normal and other high-symmetry directions, such as $\bar{\Gamma}$-$\bar{X}$, $\bar{\Gamma}$-$\bar{Y}$, and $\bar{\Gamma}$-$\bar{S}$, were determined *in situ* by means of the symmetry of the photoemission measurements and were consistent with the crystal orientation as determined via the Laue measurements. Unless stated otherwise, samples were oriented such that the angle of incidence of the x rays was approximately 40° with respect to the surface normal, with the Poynting vector and polarization vectors of x rays in the horizontal plane of the spectrometer. The sample normal was also always within a few degrees of the horizontal plane. Many different sample orientations (horizontal crystal axes versus the polarization vector of the synchrotron radiation) were utilized, to test for effects such as dependences upon polarization selectron rules. Unless stated otherwise, the sample temperatures were kept at 20 K during all operations, including cleaving and photoemission measurements. Base pressures in the experimental chamber were typically $(3-6)\times 10^{-11}$ torr, with a slight pressure jump into the 10^{-10}-torr range with activities such as cleaving of the sample. Surfaces usually remained clean for 48 or more hours under these conditions. The samples are generally temperature sensitive,[5] exhibiting marked changes of the Fermi-edge structure with cycling above T_c to about 100 K. However, some cleaved surfaces were more resilient than others and could be successfully cycled above T_c for a short time, with the Fermi-edge and 1-eV peaks serving as indicators of sample quality. Another measure of sample quality was the *absence* of the $B^F\approx 9$ eV peak from the extended valence-band (VB) spectra.[5,10] Additionally, core levels such as the 4*d* states of Ba were monitored: This is planned to be described in a future publication.[11] Samples which exhibited degradation, such as structure between 8 and 11 eV, could sometimes

be cleaned by flashing to $T \approx 100$ K. Subsequently, the quality of the sample would be verified by comparison to reference spectra. Finally, perhaps the best indication of sample quality was the "sharp" angular dependences of the acute spectral structure, an example of which is shown in Fig. 1. These angular dependences will be described in detail below. All spectroscopic characterization was complemented by optical-microscopic observation both *in situ* and particularly when the samples were removed from the vacuum chamber.

III. RESULTS AND DISCUSSION

A. Valence bands

1. VB introduction

Ascertaining the underlying foundation of the valence-band electronic structure of $YBa_2Cu_3O_{6.9}$ is a daunting task. Comparison to a general part of a predicted electronic structure is difficult because of the complexity of the calculated band structures.[12–14] The calculations give very similar Fermi surfaces. However, with 13 atoms in the orthorhombic unit cell, the calculated bands away from the Fermi level are a complex maze and differ in detail between the various calculations.[12–14] Additionally, correlation effects are clearly important, and the bands may be heavily renormalized. The parent insulator is not well described by the LDA methods utilized in Ref. 12 and 13, and it may be more appropriate to use other approaches to model the system.[15,16] Correspondingly, in the past, it has not been surprising that the photoemission spectra have exhibited a lack of distinct spectral structure in the valence bands away from the Fermi energy.

The absence of distinct and acute spectral structure in the valence bands raises an important question: Is this intrinsic or is it merely because of limitations in experimental conditions or sample preparation? For example, angular integration could result in the broad, smooth features seen in Figs. 1–4 of Ref. 5. Twinning is an obvious source of potential problems; except along $\bar{\Gamma}$-$\bar{S}$, even angle-resolved spectra would contain contributions from at least two regions of the two-dimensional Brillouin zone with further uncertainty due to the nonorthogonality of the twinning domains. On a more extrinsic level, sample deterioration or included impurities could cause signficant variations that are difficult to detect and quantify without a large number of samples. Growth defects could cause an effective spread in collection angles via the propagation of slightly askew planes. Point defects from impurities and other causes can also lower momentum resolution by degrading lattice periodicity. Stoichiometric variations, both inter- and intrasample, could cause slight changes in structures and properties that would be difficult to correlate. Many of these problems will require novel methods and enhanced capabilities to overcome, but even at this point, we are able to report the observation of acute (sharp and intense) spectral peaks in the valence bands of the cleaved surfaces of untwinned, single-crystal $YBa_2Cu_3O_{6.9}$ such as that shown in Fig. 1.

Finally, before going on to a consideration of our data, it should be noted that layer compounds such as $YBa_2Cu_3O_{6.9}$ present a special opportunity for band mapping. Because these materials are layered, it is reasonable to expect a two-dimensional or only weakly three-dimensional electronic structure.[17] Because of the fairly rigorous conservation of the photoelectron's momentum parallel to the surface during emission, angle-resolved photoelectron spectroscopy is a particularly powerful probe of two-dimensional electronic structures.[18] For three-dimensional materials, the lack of momentum conservation perpendicular to the surface during the escape of the electron from the sample means that a knowledge of the dispersion of the unoccupied final state is necessary to map the electronic structure of the bulk bands.[18] In the case of $YBa_2Cu_3O_{6.9}$, this effect is amplified by the orthorhombic unit cell.[12,19] The short real-space axes, along **a** and **b**, have lattice parameters of 3.82 and 3.89 Å, respectively. The **c** axis has a lattice parameter of 11.68 Å. Because of the finite angular acceptance of the instrument, there are typically ten resolution elements between $\bar{\Gamma}$ and $\bar{X}$ or $\bar{Y}$, but only three between Γ and Z. Combining these two conditions, it is much easier to effectively study the two-dimensional electronic structure parallel to the surface than the expectedly small changes perpendicular to the surface plane. Last, this situation also sets up a dilemma in terms of distinguishing between surface and bulk states. Generally, bulk states are three dimensional and surface states are two dimensional. Hence differentiating between two-dimensional layer and two-dimensional surface states becomes more difficult and must rely more upon gas-adsorption contamination measurements than is usual or desired. With these caveats in mind, the data will be presented and discussed.

2. VB data and discussion

The acute spectral structure at 1 eV is dependent upon both polarization and the position sampled in reciprocal space. An example of our data is shown in Fig. 2. The spectra of $\bar{X}$, $\bar{Y}$, $\bar{\Gamma}$, and $\bar{S}$ (with parallel polarization) each exhibit an intense peak near $B^F = 1$ eV. However, there are distinct differences. The very narrow peaks in the $\bar{X}$ and $\bar{Y}$ spectra each have a binding energy of 0.92 eV, with the $\bar{X}$ peak more dominant than $\bar{Y}$. Also, in both the $\bar{X}$ and $\bar{Y}$ spectra, evidence of Fermi-energy peaks can be easily seen. At $\bar{\Gamma}$ the spectrum has a much broader peak at $B^F \approx 1.3$ eV. At $\bar{S}$ the peak can be seen at an intermediate binding energy and width, with $B^F \cong 1.1$ eV in the spectrum taken with the polarization roughly parallel to the emission direction. Figure 2 also illustrates the strong polarization dependence that has been observed: If the polarization plane is perpendicular to the plane of electron collection, then a startling reduction in intensity is observed. This suggests that the 1-eV family of states is of even symmetry. Generally, one would not consider the $\bar{\Gamma}$-$\bar{S}$ plane to be a mirror plane, but if the 1-eV state is of CuO plane origin, then the $\bar{\Gamma}$-$\bar{S}$ would be almost a mirror-symmetry plane. The hypothesis of CuO plane parentage is supported by the strong similarities of the 1-eV structure at $\bar{X}$ and $\bar{Y}$: This would be unlikely for a chain-origin state. It is important to note that, although

it is now reasonable to believe that the 1-eV states at $\bar{X}$ and $\bar{Y}$ are closely related and that it is acceptable to study them with twinned crystals, this assignment and analysis would have been impossible without untwinned crystals. Before moving on, it is an important result merely that the spectra at $\bar{\Gamma}$, $\bar{S}$, and $\bar{X}$ or $\bar{Y}$ are different, unique, and of such an acute nature. This indicates the importance of the two-dimensional Brillouin zone and the real-space lattice. Ultimately, a complete description of the electronic structure must incorporate the impact of the lattice and its constituent atoms.

The high symmetry of the $\bar{X}$, $\bar{Y}$, and $\bar{S}$ points can be independently demonstrated by angle-resolved photoemission. In Fig. 3 at least two sets of peaks along $\bar{\Gamma}$-$\bar{S}$ coalesce into a single peak at $\bar{S}$. Note the symmetry as the acceptance angle is moved away from $\bar{S}$, whether toward the normal $\bar{\Gamma}$ (negative angles) or away from the normal $\bar{\Gamma}$ (positive angles). From this figure it is obvious that two or more bands are converging to $B^F \cong 1.1$ eV at the high-symmetry $\bar{S}$ point. This critical-point behavior at the zone boundary accounts for the range of widths seen at the high-symmetry points. The dispersion at Γ is even greater than at $\bar{S}$. The finite angular acceptance of the electron-energy analyzer accounts for the apparent width. The dispersion is much less near $\bar{X}/\bar{Y}$, and the experimental widths are correspondingly much narrower. The data near $\bar{X}$ are shown in Fig. 4. Here a peak can be seen to grow out of the higher-binding-energy "background," as the collection angle moves toward $\bar{X}$. At $\bar{X}$ a narrow peak (full width at half maximum of 0.15 eV) can be seen at $B^F \approx 0.92$ eV. The spectra shown in Fig. 4 are mainly for a rotation beyond $\bar{X}$, along $\bar{\Gamma}$-$\bar{X}$-$\bar{\Gamma}$, but away from the sample normal $\bar{\Gamma}$. Additional data along $\bar{\Gamma}$-$\bar{X}$-$\bar{\Gamma}$, but toward the sample normal $\bar{\Gamma}$, as well as a perpendicular rotation, all show similar effects: the emergence of a peak from a rising background, which has an onset at $B^F = 0.9$ eV. In light of the $\bar{S}$ data in Fig. 3 and the asymmetry of the peaks in Fig. 4, it seems plausible that a convergence of two bands may also be occurring at $\bar{X}$. It is also easy to see how the combination of poorer resolution and slight misalignment from a high-symmetry direction could give rise to a line shape similar to that of a Fano resonance.[20] Additionally, it is intriguing to compare these photoemission peaks to the momentum-dependent electron-energy-loss spectra, which also exhibit an intense and narrow feature.[21] In any case, strong symmetry of emission and extrema behavior is seen at $\bar{S}$, $\bar{X}$, $\bar{Y}$, and $\bar{\Gamma}$. Although these peaks and the corresponding electronic structures are of interest in themselves, they also serve a very useful purpose: Having been mapped in detail, their extreme angle sensitivity allows a rapid determination of crystal orientation *in situ*. Next, the dispersion of the 1-eV state near $\bar{X}$ will be considered

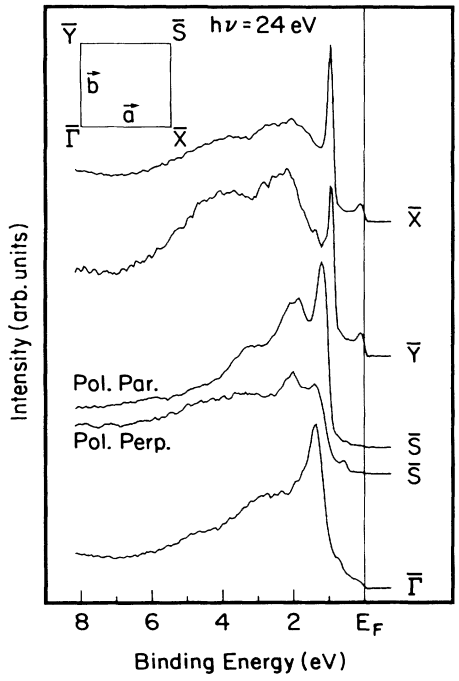

FIG. 2. This figure illustrates the family of peaks near $B^F = 1$ eV at $\bar{\Gamma}$, $\bar{S}$, $\bar{X}$, and $\bar{Y}$. Note the variation in peak position, height, and width for $\bar{\Gamma}$, $\bar{S}$, $\bar{X}$, and $\bar{Y}$. Also, a strong polarization dependence has been observed. Fermi-energy peaks are present in the $\bar{X}$ and $\bar{Y}$ spectra, but not the $\bar{S}$ and $\bar{\Gamma}$ spectra. The two-dimensional Brillouin zone is obtained by collapsing the three-dimensional zone along **C**. Thus Γ-Z becomes $\bar{\Gamma}$, X-U becomes $\bar{X}$, Y-T becomes $\bar{Y}$, and S-R becomes $\bar{S}$. A schematic of the two-dimensional Brillouin zone is shown as an inset, illustrating the relationships between primitive vectors (**a** and **b**) and zone boundaries (e.g., $\bar{X}$ and $\bar{Y}$).

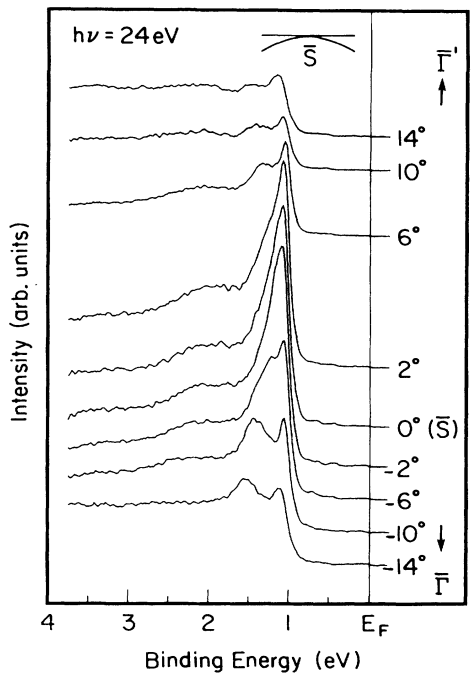

FIG. 3. Spectra shown here were collected near the $\bar{S}$ point of the Brillouin zone using $h\nu = 24$ eV. Unlike the other spectra shown in this paper, these were taken using a twinned $YBa_2Cu_3O_{6.9}$ crystal. A similar though not as extensive set was collected using an untwinned crystal. Note the coalescence of two peaks into a single peak at $\bar{S}$. At $\pm 14°$ rotation away from $\bar{S}$, the region of reciprocal space that is sampled is roughly halfway between $\bar{\Gamma}$ and $\bar{S}$.

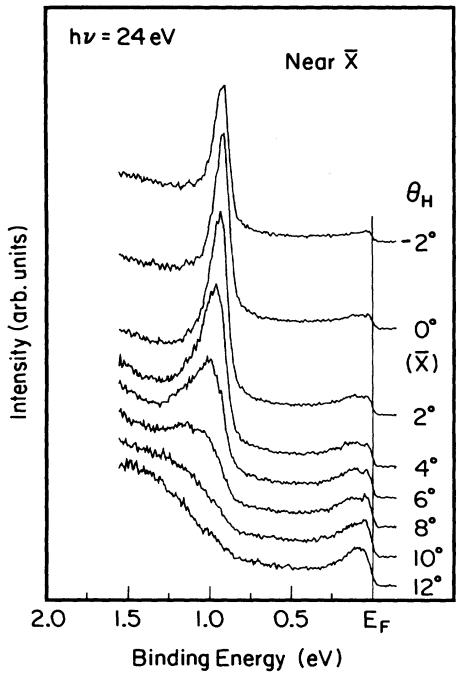

FIG. 4. These spectra were taken with $h\nu=24$ eV and near $\bar{X}$ in the two-dimensional Brillouin zone. They demonstrate the acute nature of the peak near $B^F=0.92$ eV at $\bar{X}$ and also the dispersion of the peak away from $\bar{X}$. The peak has a full width at half maximum of 0.15 eV at $\bar{X}$. Using 24-eV photons, there is an angular separation of 21° between $\bar{\Gamma}$ and $\bar{X}$.

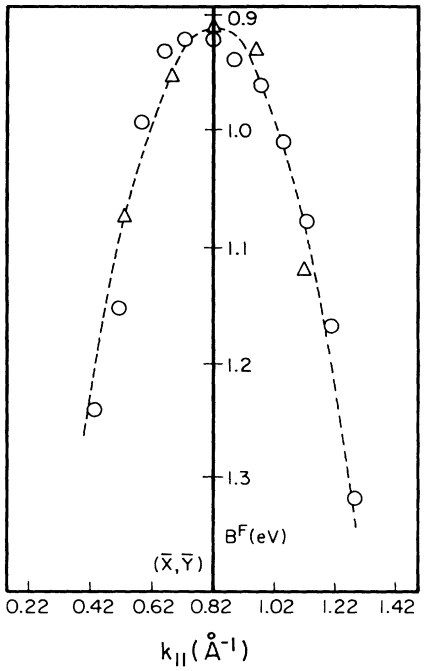

FIG. 5. Dispersion curve plots for the 1-eV state near $\bar{X}$ are shown here. The data for $h\nu=24$ eV (open circles) were taken using an untwinned crystal. The data for $h\nu=74$ eV (open triangles) were collected using a twinned crystal. Thus only $\bar{X}$ was probed at $h\nu=24$ eV, but both $\bar{X}$ and $\bar{Y}$ were contributing at $h\nu=74$ eV. These dispersion curves are taken from the peak maxima: At this point we are unable to resolve unambiguously the hypothesized two components, as illustrated in the inset of Fig. 3. The ratio of the effective mass to the rest mass of an electron is -2 for the curve shown in this figure.

more carefully.

The 1-eV state at $\bar{X}$ exhibits a strong, two-dimensional dispersion. Shown in Fig. 5 is the dispersion curve approximately along $\bar{\Gamma}$-$\bar{X}$-$\bar{\Gamma}$. The $h\nu=24$ eV data were collected using an untwinned, single crystal of $YBa_2Cu_3O_{6.9}$ (an example of which is shown in Fig. 4). The dispersion is symmetric about $\bar{X}$ and quite strong, with the binding energy of the peaks centroid changing by 0.4 eV over about $\frac{1}{2}$ the separation of $\bar{X}$ from $\bar{\Gamma}$. A similar, if not identical, dispersion curve was subsequently observed, using a twinned crystal and $h\nu=74$ eV. The independence of the dispersion from photon energy (and thus perpendicular momentum) is strong evidence that the electronic structure is truly two dimensional, not three dimensional. Additionally, dispersion curves perpendicular to the $\bar{\Gamma}$-$\bar{X}$-$\bar{\Gamma}$ line, approximately along $\bar{S}$-$\bar{X}$-$\bar{S}$, were measured using $h\nu=24$ and 74 eV. Again, the data from the two different photon energies agreed, showing symmetric dispersion to higher binding energy when moving away from $\bar{X}$. The dispersion along $\bar{S}$-$\bar{X}$-$\bar{S}$ was substantially weaker than that along $\bar{\Gamma}$-$\bar{X}$-$\bar{\Gamma}$. Thus it can be seen that the dispersion of the 1-eV state is two dimensional: Dependent upon parallel momentum, but independent of photon energy and perpendicular momentum.

While the dispersion does not vary with photon energy, the *cross section* of the 1-eV state at $(\bar{X},\bar{Y})$ does. In Fig. 6 are a series of spectra, taken with photon energies over the range 14–74 eV. There are large fluctuations in the relative intensity of the peak at 1 eV over this range, with large intensity at $h\nu=24$ and 74 eV and weak signals at $h\nu=14$ and 50 eV. There are also variations in the intensity of the peak at the Fermi level: It is an important result that the modulations of the intensities of these two peaks, at $B^F\approx 1$ and $\cong 0$ eV, are out of phase. It argues against a common origin for the 1-eV and Fermi peaks, for example, two different screening states, a photoemission many-body satellite,[22] or an extrinsic plasmon coupling.[21] (From our data set, it is not possible to completely rule out possibilities such as an antiphase relationship between the Fermi and 1-eV peaks or a complex intrinsic plasmonic coupling.) Additionally, the two regimes of high intensity, near $h\nu=24$ and 74 eV, correspond to final-state crystal momenta of about 2.8 and 4.6 Å^{-1}, respectively. While we have not pursued these measurements to photon energies above 74 eV, it is interesting that the crystal momentum has approximately doubled in going from one maxima regime to another. This is consistent with observations concerning the cross-section variations of two-dimensional surface states.[23] It is reasonable that spatially confined, two-dimensional layered states would experience cross-section modulations similar to those observed in spatially confined, two-dimensional surface states. Thus this strong photon-energy dependence does not seem to be a resonance, an atomic cross-section effect, or due to direct linkage with the Fermi peak, but rather a matrix-element effect that may be due to the two-dimensional nature of the state.

Before going on to a consideration of why this state is

not a surface state, it should be noted that there does seem to be some "resonant" behavior in this peak, superimposed on the broader energy dependence described above. Crossing the threshold for the Cu $3p$ cores, $h\nu \cong 72$ eV, results in an enhancement at $(\bar{X}, \bar{Y})$, but none away from $(\bar{X}, \bar{Y})$. This is shown in panel (A) of Fig. 7. (Not shown is the expected and observed resonance of the 12-eV satellite.) This suggests that the 1-eV state has fairly pure Cu character at the zone boundary $(\bar{X}, \bar{Y})$, but that it is heavily hybridized away from the zone boundary. (Note also that no resonance is seen in the Fermi-edge structure at either position in reciprocal space, another example of the lack of linkage between the 1-eV and Fermi peaks.) The data shown in Fig. 7 is consistent with our hypothesis that the 1-eV state is associated with the CuO planes.

It is tempting to think of the 1-eV states as "surface states,"[23] but we believe this to be incorrect despite the preliminary indications of a study done using twinned crystals and a resonance lamp.[10] First, the entire band structure is strongly two dimensional, and so two dimensionality does not automatically imply a nonbulk nature. Second, the 1-eV peak appears to be independent of the terminating layer. Panel (B) of Fig. 7 shows the possible terminations if cleavage occurs at a Ba-O plane. The consistent appearance of the state argues against its origin in the interface of vacuum and a specific layer. This is reinforced by studies correlating Ba core spectra with strengths of other core levels and relative strengths of valence-band features. This is planned to be discussed in a future publication.[11] Third, the state does not exist in a gap of the bulk band structure, thus, at best, it would be a surface resonance. Fourth, the state exists over a wide part of the Brillouin zone (BZ), for example, as seen in Figs. 4 and 5. This suggests that it is intrinsic to the material. Fifth, gas-absorption measurements point toward limited surface sensitivity. As the sample deteriorates,

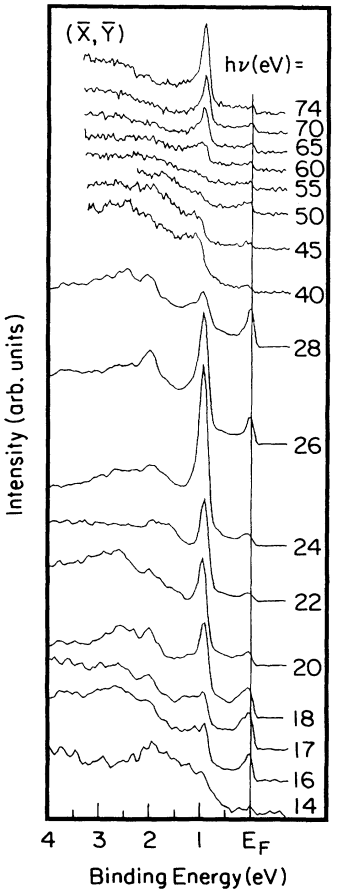

FIG. 6. Photon-energy dependences of the 1-eV and Fermi states near $(\bar{X}$ and $\bar{Y})$ are illustrated here. A twinned crystal was used for this measurement. Note the large resonances of the 1-eV peak at $h\nu = 24$ and 74 eV.

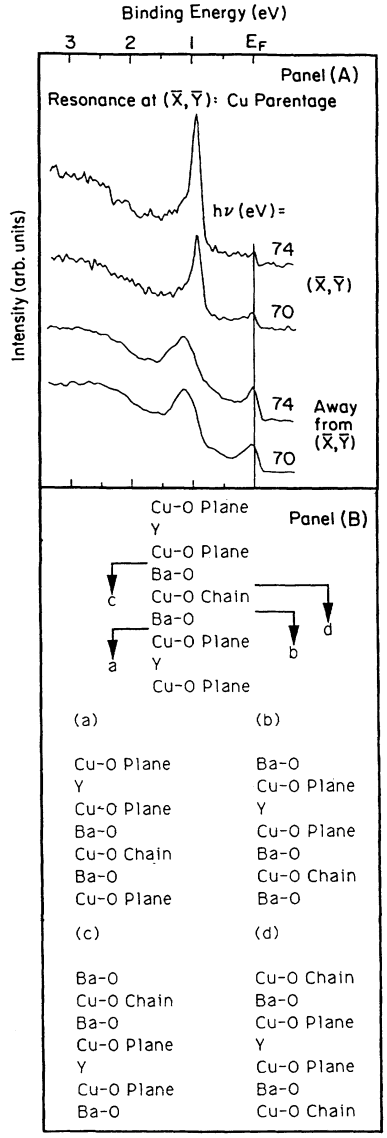

FIG. 7. Panel (A): Resonance behavior of the 1-eV peak is shown here. Two sets of spectra, one each at $h\nu = 70$ eV (below the Cu $3p$ threshold) and the other at $h\nu = 74$ eV (above the Cu $3p$ threshold), for $(\bar{X}$ and $\bar{Y})$ and away from $(\bar{X}$ and $\bar{Y})$, are compared. Note the enhancement of intensity for $h\nu = 74$ eV at $(\bar{X}$ and $\bar{Y})$. Panel (B): Shown here are some possibilities for cleavage planes in $YBa_2Cu_3O_{6.9}$. See the text for details.

there is degradation of the 1-eV peak. However, gas-adsorption studies with O_2, Ar, and other gases do not show any preferential sensitivity by the 1-eV peak. Both the Fermi-energy and 1-eV peaks attenuate, but neither is overwhelmingly sensitive to gas deposition. It is reasonable to expect attenuation of all photoemission valence-band structures with gas adsorption, owing to the short mean free paths at these photon energies. Additionally, generic degradation of the spectra is to be anticipated with sample deterioriation over time and with exposure to contamination.

The 1-eV state is an acute spectral structure observed in the valence bands away from the Fermi energy and is important on two counts. Scientifically, it does not appear to be a surface state, but rather is intrinsic to the material. Thus it is a challenge to various theoretical modeling methods to explain its behavior, providing a clear-cut measure of success or failure. It may be the lattice-modified result of a lower Hubbard band[16] or the states split off from the remnant of the CuO_2 bands, into what was once the insulator band gap.[12–15] This picture is appealing, in analogy to surface states in three-dimensional metals and semiconductors. The surface states are caused by the perturbation to the bulk potential, which arises because of truncation of the bulk lattice. In our case the disturbance could be chemical, in that the doping causes a perturbation upon the parent copper oxide. Thus the states would exist in what was the CuO_2 insulator gap, but not a gap associated with bulk $YBa_2Cu_3O_{6.9}$. Regardless of the final outcome, this family of states provides a solid benchmark for comparison to theory. In the case of modifications to LDA calculations, the energy shift of specific parts of the band structure can be tested. In the case of models starting from a Hubbard band, there is a quantitative test of the modifications due to the periodic lattice. The binding energies vary by 0.4 eV, and dispersions of up to 0.5 eV are seen. Technologically, this state now becomes the measure of surface quality. In much the same vein as the O 1*s* core spectra for unordered samples, the 1-eV peaks at $\bar{X}$, $\bar{Y}$, and $\bar{S}$ now are the standard for near-surface quality in terms of purity and ordering, i.e., the indication of a high-quality sample.

B. Fermi surface

1. Introduction

The determination of the Fermi surface requires the best possible samples and highest resolution. An example of our data, using cleaved, untwinned single crystals of $YBa_2Cu_3O_{6.9}$ at 20 K, is shown in Fig. 8. High-quality samples are necessary to see any strength or sharpness near the Fermi edge. The spectra from evaporated thin films at room temperature exhibit none of this detailed structure.[4] In fact, it is extremely unlikely that the peak in Fig. 8 could even be resolved at room temperature: The 10%–90% Fermi-edge widths of conductors is 113 meV at room temperature, almost 3 times as wide as the peak in Fig. 8. Even the earlier study[3] using twinned single crystals does not have such sharp and well-defined spectral structure, leading to doubts about assignments as well as sample quality. Moreover, the best twinned samples and their spectra are inherently compromised: It is impossible to uniquely define the location of emission in k space, save for along the $\bar{\Gamma}$-$\bar{S}$ line. It is of interest that the study done with twinned samples shows the possibility of fairly good agreement with the theoretical predictions of a local-density-approximation calculation.[12] A very recent study with high-angular-resolution and twinned crystals reported partial agreement.[10] Nevertheless, the artificial symmetrization caused by twinning not only causes an overlay of nonequivalent sites (e.g., $\bar{X}$ and $\bar{Y}$), but also may contribute to a smearing of the structure because of the slight nonorthogonality of the two twinned domains.[19] It is unclear how close to the $\bar{\Gamma}$-$\bar{S}$ line these deleterious effects extend. An important goal of photoemission investigations of $YBa_2Cu_3O_{6.9}$ is the separation of the contributions of the one-dimensional chain states from the two-dimensional plane states, which inherently requires a differentiation of the $\bar{X}$ side of the BZ from the $\bar{Y}$ side of the BZ.

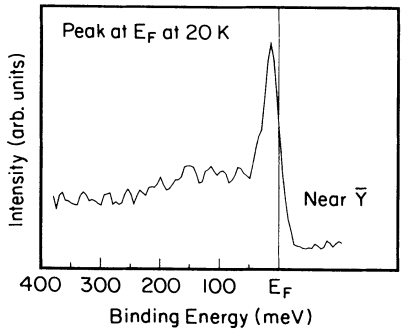

FIG. 8. Shown here is a spectrum taken from untwinned, single-crystal $YBa_2Cu_3O_{6.9}$, near the high-symmetry point $\bar{Y}$. Note the sharp and intense peak near the Fermi energy. This peak is not observed at $\bar{X}$. The peak has a total full width at half maximum of about 40 meV, including an instrumental broadening of about 30 meV. The photon energy was 17 eV.

Comparison in a momentum-resolving mode of photoemission-band mapping with band-structure calculations is an important and useful operation, if only possibly to ascertain which states are normal and which are not, i.e., superconducting. Both the experimental and theoretical sides of this comparison are rife with limitations, but there has been a fairly extensive history of success in a variety of systems.[24] In the case of $YBa_2Cu_3O_{6.9}$, we are further encouraged by what seems to be a high level of agreement between the various computational results.

Despite the general overall agreement of the theoretical results of Refs. 12–14, some small, yet significant differences exist. All three calculations show three bands (1, 2, and 3 of Ref. 12) which cross the Fermi energy along X-S and Γ-S, having roughly the same topography throughout the zone. A major point of difference though is the behavior of the chain-derived fourth band (No. 4 of Ref. 12), which may or may not cross the Fermi energy. Massida and co-workers[12] show band 4 as weakly dispersive and fluctuating across the Fermi energy all along Γ-Y-S. Pickett, Cohen, and Krakauer[13] do not have this

crossing along Γ-Y, although they do show a potential pocket in the Fermi-surface map around S, similar to Massida and co-workers. This pocket has apparently been seen in recent de Haas–van Alphen measurements.[25,26] The calculation by Hirao, Uda, and Murayama[14] has an intermediate result, with a band skimming along ΓY just below the Fermi energy. (Hirao, Uda, and Murayama also see a weakly dispersive band at $B^5 \approx 0.5$ eV, which may be the cause of the weak feature at $B^F \approx 0.5$ eV in the $\bar{S}$ spectra of Fig. 2.) Pickett, Cohen, and Krakauer emphasize the importance of the third dimension (along **c** perpendicular to **a** and **b**) in their calculation, producing a two-dimensional map of Fermi crossings which integrates contributions along the **c** direction. Nevertheless, there is a strong retention of two dimensionality and a similarity to the calculated Fermi surfaces of Massida and co-workers and the Fermi surface of each band remains fairly well separated from each other. Experimentally, the effective broadening of the Fermi surface of Pickett, Cohn, and Krakauer is roughly equivalent to the sampling area in momentum space of these measurements. Thus it is quite a challenge to the experimentalist to differentiate between these models, with the $\bar{Y}$ region being perhaps the most promising candidate. Additionally, our samples are $O_{6.9}$, while the calculations are O_7: It is necessary for us to anticipate oxygen-depletion effects upon the band structure.[12] Finally, before going on to a consideration of the data, it is encouraging to note the recent results of Haghighi *et al.*,[27] in which the existence of the Fermi surface of room-temperature $YBa_2Cu_3O_{6.9}$ has been conclusively demonstrated with the technique of positron annihilation.

2. *Fermi-surface data and discussion*

A summary of our Fermi-surface mapping is shown in Fig. 9(a): We are concentrating upon the regions near $\bar{X}$ and $\bar{Y}$, to separate contributions from the chain- and plane-derived states. This is a purely empirical construction, using Laue backscattering and symmetry in the photoelectron spectra to determine crystal alignment and presuming that momentum is conserved parallel to the surface, in the (**a**,**b**) plane. Before prejudicing our analysis by a comparison with band-structure calculations, the crossings along each line will be discussed.

The spectra from near $\bar{Y}$ shown in Fig. 10 are remarkable in the sharpness of the peak at the Fermi energy and the apparent lack of dispersion. It appears that, as the emission direction is varied, the peak attenuates instead of dispersing. These peaks have a total FWHM of 40 meV, with an instrumental contribution of 30 meV. Thus the peak width and shape are dominated by instrumental considerations, and the lack of dispersion has the effect of generating the rare situation where energy resolution alone is the limiting factor. It is important that this sharp feature is observed only at $\bar{Y}$: It is not seen at $\bar{X}$, as is illustrated by Fig. 11.

The data in Fig. 11 establish three important points. (1) There is symmetry about the $\bar{\Gamma}$-$\bar{X}$ axis, as seen by the crossings on both sides of $\bar{X}$, along $\bar{S}$-$\bar{X}$-$\bar{S}$. (2) There is significant intensity at the Fermi energy near $\bar{X}$ well away

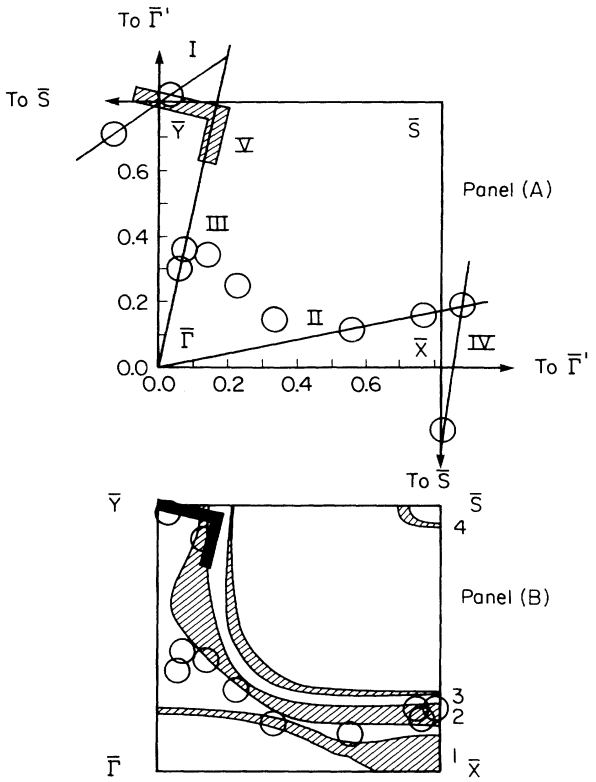

FIG. 9. Fermi surface mapping of $YBa_2Cu_3O_{6.9}$ is shown here. In panel (A), the experimental paths through the zone are shown, in the spirit of an extended-zone scheme. Crossings are denoted with a circle whose size indicates the system resolution. Panel (B) Folded inside the reduced or first zone, the crossings are compared to the calculations of Pickett, Cohen, and Krakauer (Ref. 13). The bands are labeled as in Massida and co-workers (Ref. 12), who assign (1) and (4) as chain derived and (2) and (3) as plane derived.

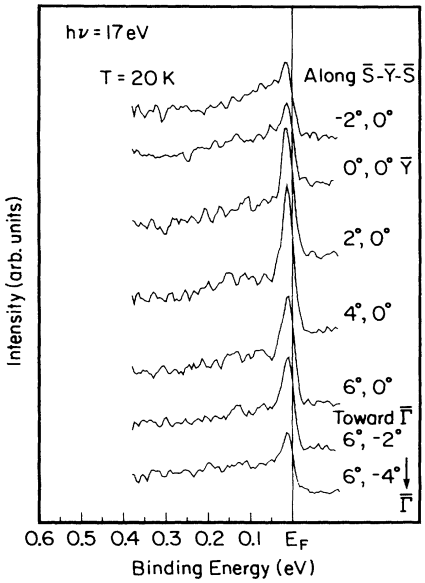

FIG. 10. Spectra shown here were collected near the high-symmetry point $\bar{Y}$, with the rotation approximately along $\bar{S}$-$\bar{Y}$-$\bar{S}$. The light polarization and emission direction were fairly well aligned and the photon energy used was 17 eV. These data are shown as line (v) in Fig. 9.

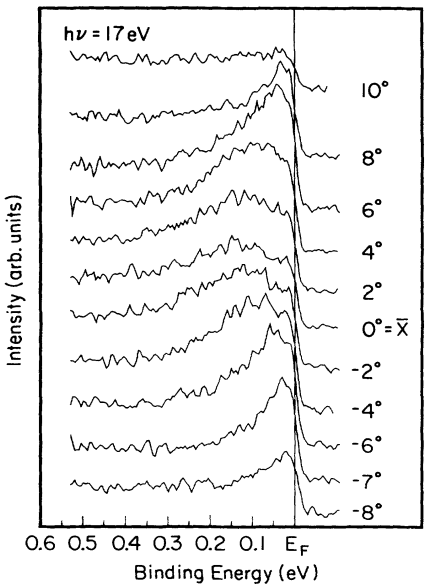

FIG. 11. Spectra collected near $\bar{X}$ using 17-eV photons are plotted here. The rotation was approximately along $\bar{S}$-$\bar{X}$-$\bar{S}$, as shown in Fig. 9 as line (iv). The emission direction and light polarization were fairly well aligned. The ratio of the effective mass to the reduced mass for the data shown here is approximately 1.6.

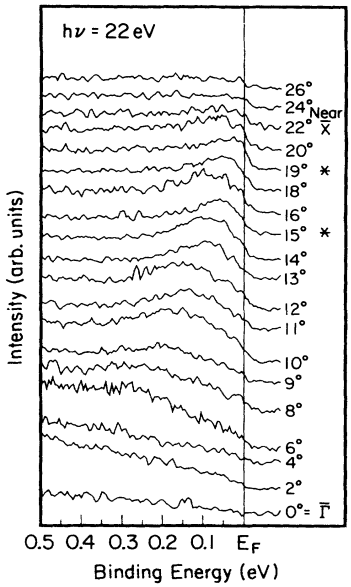

FIG. 12. These data are spectra collected with $h\nu=22$ eV light with electron emission in a plane that is 12° away from the $\bar{\Gamma}$-$\bar{X}$ axis. The polarization vector of the light and emission direction of the electrons are poorly aligned. These data are shown as line (ii) in Fig. 9.

from and between the other crossings. (3) The peak seen in Figs. 8 and 10 is specific to $\bar{Y}$: It is not seen at $\bar{X}$. The conditions of the experiment are very similar, almost identical, for Figs. 10 and 11. The emission directions are aligned with the light polarization, the photon energies are the same, and the emission angles relative to the surface normal are almost identical. Once again, the untwinned crystals allow us to discern a level of detail that is otherwise lost, and the inequivalence of the **a** and **b** axes is confirmed.

The issue of multiple bands and crossings is probably best addressed by considering the data in Figs. 12 and 13, where two crossings each are observed. In Fig. 12, moving along from $\bar{\Gamma}$ to near $\bar{X}$, a large broad peak can be seen dispersing to lower binding energies. Eventually, two components can be seen near $B^F \approx 0.05$ and 0.15 eV, which then individually and sequentially cross the Fermi energy as the electron momentum is moved closer to $\bar{X}$. A similar series of events can be seen along $\bar{\Gamma}$-$\bar{Y}$ in Fig. 13, although the states are not as well resolved and the crossings are closer to $\bar{\Gamma}$ along $\bar{\Gamma}$-$\bar{Y}$ than $\bar{\Gamma}$-$\bar{X}$. Additionally, it appears that in Fig. 13 significant intensity may be observed near the Fermi energy at larger angles, toward $\bar{Y}$ with a skewing along $\bar{Y}$-$\bar{S}$ from the 12° misalignment, as shown in Fig. 9. This is suggestive of another crossing.

Figure 14 shows spectra on either side of $\bar{Y}$, approximately along an $\bar{X}$-$\bar{Y}$-$\bar{X}$ axis. The crossings are similar to those observed near $\bar{X}$ in Fig. 11. Note that these spectra and Fig. 13 do not show the extremely sharp peak near $\bar{Y}$ that dominates Figs. 8 and 10. The experimental difference among these spectra is not sample quality or variation, but photon energy. (There is some difference in the polarization direction relative to the emission and rotation direction, but these are not the dominant contributions in this case.) This is a dramatic example of the phenomena illustrated in Fig. 6: Individual features in the photoemission spectra exhibit very strong photon-energy-dependent matrix-element effects. This can be a sobering effect. Just because a feature is not seen at a given orientation and photon energy does not mean it does not exist. On the positive side, the same depen-

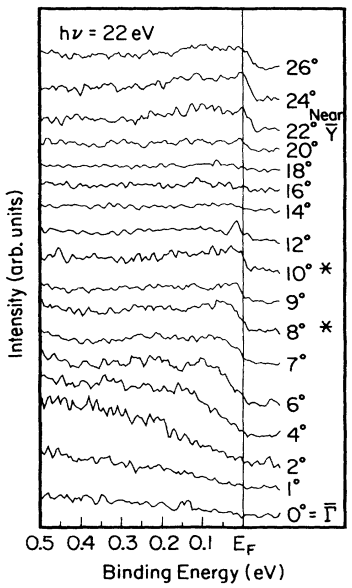

FIG. 13. Data shown here are spectra collected with $h\nu=22$ eV light and with emission directions in a plane that is 12° away from the $\bar{\Gamma}$-$\bar{Y}$ axis. The polarization of the light and emission directions were fairly well aligned toward $\bar{Y}$. These data are shown as line (iii) in Fig. 9.

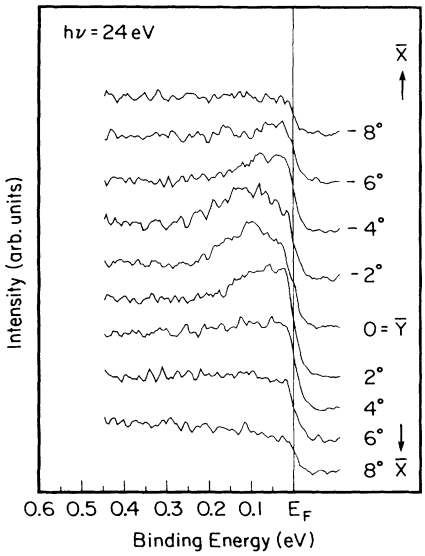

FIG. 14. Shown here are spectra taken with $h\nu = 24$ eV near the $\bar{Y}$ point, along and $\bar{X}$-$\bar{Y}$-$\bar{X}$ axis. The polarization is only partially aligned with the emission direction, with the rotation plane at roughly 36° from the plane containing the light polarization. This is shown as line (i) in Fig. 9.

dences allow weak features to be seen by the suppression of stronger transitions. This is illustrated in the comparison of Figs. 8 and 14. The unresolved structure near 100 meV in the spectrum of Fig. 8, taken at 17 eV, can be studied in detail at 24 eV, as seen in Fig. 14. This peak may be another band.

In addition to the crossings along the lines discussed above, Fig. 9 shows three crossings in what should be the symmetric part of the zone near the Γ-S line. This data come from a sample oriented with the Γ-S axis roughly aligned with the polarization vector. (In this geometry band 3 is not seen. In contrast, Mante and co-workers[10] using unpolarized light, report a crossing at band 3, but are unable to resolve the band-2 crossing. Liu *et al.*,[28] see both crossings.)

The spectra reported in this paper are representative of those from a large number of samples, oriented with a variety of polarization angles and studied systematically over the phonon-energy range 15–30 eV. While there is much detailed work to be done, we feel that the general picture is becoming clear. From the spectra and plots shown in Figs. 9–14, it is obvious that the Fermi-surface electronic structure of $YBa_2Cu_3O_{6.9}$ does not have fourfold symmetry about the surface normal, thus establishing the inequivalence of the $\bar{\Gamma}$-$\bar{X}$ and $\bar{\Gamma}$-$\bar{Y}$ directions of the Fermi surface. But the question arises, what can be said about band parentage, i.e., chain versus plane origin, without resorting to comparison to the calculated bands?

This question has been addressed by correlating the behavior of the Fermi-edge peak near $\bar{Y}$ of Figs. 8 and 10 with core-level measurements, particularly the Ba 4*d* peaks: The data suggest that the $\bar{Y}$ peak is particularly strong if a specific core spectrum is observed. Preliminarily, we associate this core spectrum with a cleavage structure (one of four possibilities) which would expose a chain structure on the outermost surface plane [(d) in panel (B) of Fig. 7]. In this model, however, the Fermi-energy peak (like the 1-eV peak) is not a surface state; rather, it is a layer state which has a maximization of intensity by placing that layer on the surface. This is consistent with our observation of the Fermi-energy peak at $\bar{Y}$ with different samples, cleaves, and Ba 4*d* core spectra. The other cleavage terminations would have the chain layer buried inside the $YBa_2Cu_3O_{6.9}$ lattice: Hence a lack of great sensitivity to Ar and O_2 adsorption is not unreasonable, even for the chain-layer-terminated cleave. This is because of the apparent insensitivity of the Fermi-energy state to the presence or absence of an adjoining layer, whether it be from the $YBa_2Cu_3O_{6.9}$ structure or condensed Ar or O_2. This subject and particularly the Ba 4*d* core-level spectra are planned to be discussed in a future publication.[11] Finally, before going on to a comparison with theory, the hypothesis of chain derivation of this Fermi-energy peak is also supported by some recent work done in which the oxygen content of twinned crystals has been varied.[28]

Next, the experimental Fermi crossings and spectra will be compared to the theoretical band structures. Figure 9(b) is an overlay of our Fermi-band crossings and the calculated Fermi surface of Pickett, Cohen, and Krakauer[13] summed over the c direction. It is immediately obvious that there is remarkably good agreement in the region along $\bar{\Gamma}$-$\bar{X}$, near to $\bar{X}$. Remember, our experimental resolution is about 10% of the $\bar{\Gamma}$-$\bar{X}$, $\bar{Y}$ distance. Crossings are seen for both plane and chain bands. Along line (ii) only two crossings are seen: It appears that the scans were terminated before getting to band 3. It also seems fairly likely that it will be almost impossible to separate the adjacent bands (2) and (3) even by scanning along this favorable direction. Line (iv) spectra of Fig. 11 shows a substantial Fermi-edge strength around $\bar{X}$ and inside the crossings. This may be indicative of an unresolved crossing of band (1) and possibly (2). It may also be an indication of the k_z smearing predicted by Pickett, Cohen, and Krakauer.[13] The data along the $\bar{\Gamma}$-$\bar{Y}$ direction do not agree as well with theory. Line (iii) has two crossings, one which agrees well with band (2), plane derived, and the other which is probably band (1), chain derived, but at a slightly different location in the BZ than that predicted by Pickett, Cohen, and Krakauer[13] for O_7. The other Fermi-energy intensity of the line (iii) spectra, toward the end of the line away from $\bar{\Gamma}$, may be associated with band 2 or 3. The crossings of lines (i) and (v), near $\bar{Y}$, are the most problematic.

From the spectra of Figs. 8, 10, and 14, it seems as though the state near $\bar{Y}$ is not so much dispersing toward or away from the Fermi energy as it is merely varying in intensity, with the peak at or near (within 10 meV or less) the Fermi energy. (Peak fittings will be discussed in the third section on gaps.) This is probably band 4, particularly as calculated by Hirao, Uda, and Murayama[14] or Massida and co-workers[12] if oxygen depeletion from $x = 7$ to 6.9 moves the Fermi energy up slightly, as Massida and co-workers suggest. It is also of note, as mentioned above, that we may be seeing the 0.5-eV feature of Hirao, Uda, and Murayama in some of our spectra (Fig. 2).

At this point the question arises whether it will be possible to separate out $\mathbf{k}_z$ dependences. With the data that we have in hand now, the answer is no. Nevertheless, it is conceivable to design experiments in which photon energies and angles are changed incrementally, keeping the position in the two-dimensional BZ of the **a**-**b** plane fixed. This will be a difficult experiment for two reasons. First, the final-state structure is unknown, and so all positioning in k_z space will be relative. Second, the angular resolution requirements will be severe. Using similar estimates for $\mathbf{k}_z$ as for the momentum parallel to the plane, we currently resolve $\frac{1}{3}$ of the BZ along the c axis. This represents the bare minimum of that which is necessary.

To summarize, we have seen the following: (1) well-defined crossing of the Fermi energy along $\bar{\Gamma}$-$\bar{X}$ and $\bar{\Gamma}$-$\bar{Y}$, which unequivocably establish the asymmetry of the Fermi electronic structure parallel and perpendicular to the chain direction (**b** or $\bar{\Gamma}$-$\bar{Y}$), and (2) an agreement with band-structure calculations, which, in turn, provides experimental support for the computationally based assignment of chain features. The observation of a Fermi-band crossing with sharp, well-defined peaks at a temperature of 20 K raises the last and probably most important issue: The existence and magnitude of the superconducting gap.

C. Superconducting gap

1. *Introduction*

One of the most important measurements with respect to the properties of high-temperature superconducutors is that of the width of the superconducting gap: Unfortunately, in $YBa_2Cu_3O_{6.9}$ there is substantial confusion concerning this property. For example, consider the following. Infrared spectroscopy measurements[29] of the gap associated with the CuO planes indicate gaps of $2\Delta_{a,b}=8kT_c$ ($\sim$60 meV) and $2\Delta_c=3kT_c$ (24 meV). Tunneling measurements[30] also suggest a double-gap structure[31], $2\Delta_{a,b}=39$ meV and $2\Delta_c=8$ meV, with both a nonzero conductance at zero bias and a linear background conductance near zero bias. The subscripts a, b, and c are to distinguish between gaps associated with being parallel (a,b) and perpendicular to the planes containing the a and b axes. NMR experiments[32] indicate a two-gap structure as well. Here, however, the gaps are assigned to the CuO plane states ($2\Delta=3.8k_BT-6.2k_BT$ or 29–48 meV) and the CuO chain states ($2\Delta=3.52k_BT=27$ meV). Raman measurements also point to a two-gap structure,[33,34] with $2\Delta_{a,b}=6.8$ to $7.7kT_c$ (53–60 meV) and $2\Delta_c=3.5kT_c$ (27 meV). Additionally, there are measurements which suggest that there is electronic density inside the superconducting gap. This includes specific-heat measurements,[35] Raman-scattering experiments,[36] and microwave-resistivity determinations.[37] Angle-resolved photoelectron spectroscopy represents an attractive means of unraveling this problem, because of its capability to probe directly the occupied electronic states in a momentum-resolving mode. Previous photoemission measurements[3] have been unable to properly address these issues, because of inferior samples (e.g., twinning) and poorer resolution (100 meV or more). Despite preliminary reports of a large gap (25 meV),[7] our measurements, using *untwinned,* single-crystal $YBa_2Cu_3O_{6.9}$ and with an energy resolution (full width at half maximum) of 30 meV and an angular resolution of $\pm1°$, are not consistent with a gap greater than 10 meV ($\Delta\leq5\pm5$ meV). Mante and co-workers[10] have recently reached the same conclusion using higher angular but lower-energy resolution and twinned crystals of slightly lower oxygen concentration. Several hypotheses concerning the lack of observation of a large gap in $YBa_2Cu_3O_{6.9}$ with photoemission and addressing the seeming inconsistencies of the above various measurements will be discussed. Additionally, a description of physical differences between $Bi_2Sr_2CaCu_2O_8$ and $YBa_2Cu_3O_{6.9}$ will be presented, which may help to explain why a gap is seen with photoemission in the former but not the latter.

2. *Gap data and discussion*

The central result of this part of the investigation is that our photoemission measurements indicate the absence of a large gap in all of our Fermi-surface measurements. This includes both the bands assigned as chains and planes, as based upon comparison with LDA calculations. An upper-bound estimate of the gap is approximately $\Delta\leq5$ meV; 2Δ may be significantly smaller than 10 meV. Looking at the spectra of Fig. 10–14, it can be seen that each crossing exhibits a shoulder or peak near the Fermi energy, with the Fermi energy well up the side of the shoulder or peak. This is the indication of an apparently small or zero gap, as will be described next.

To demonstrate that the placement of the Fermi energy on the peak or shoulder of the spectral feature is an indication of a small gap, two arguments will be made. First, a comparison with $Bi_2Sr_2CaCu_2O_8$ and, second, an analysis of the spectral features will be made.

A series of spectra are shown in Fig. 15: (a) $YBa_2Cu_3O_{6.9}$ at 100 K, (b) $YBa_2Cu_3O_{6.9}$ at 20 K, and (c) Pt at 20 K. These spectra were taken sequentially [(a), (b), and then (c)], with no adjustments to the apparatus other than to cool the samples between (a) and (b) and to move the sample holder between (b) and (c). [A spectrum taken before warming agrees with spectrum (b) taken after warming.] Note how the Fermi energy runs through the middle of the rise in spectra (a) and (c), but is adjacent to the peak in spectrum (b). If this figure is compared to the spectra of $Bi_2Sr_2CaCu_2O_8$ in Fig. 2 of Ref. 2, the differences are startling. For $Bi_2Sr_2CaCu_2O_8$ at 20 K, the peak near the Fermi energy is approximately 40 meV from the Fermi energy, which crosses the spectrum at the beginning of the rise, not the end. In Fig. 15 the spectrum of $YBa_2Cu_3O_{6.9}$ at 20 K has a peak within approximately 10 meV of the Fermi energy.

Although the peak position is not a direct measure of the gap, it is indicative. $Bi_2Sr_2CaCu_2O_8$ has a gap (Δ) of 24 meV. If the natural line shape and experimental instrument functions were the same, this would indicate a near-zero gap for $YBa_2Cu_3O_{6.9}$. To ascertain more accurately the magnitude of the gap, the specifics of the near-Fermi-energy measurements must be considered. There

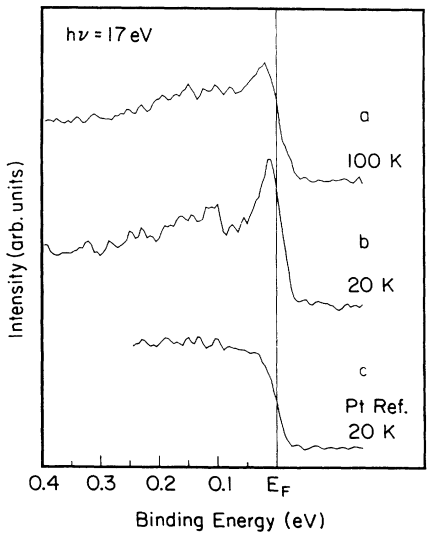

FIG. 15. Series of high-resolution spectra are shown here, where nothing has been changed except to cool the $YBa_2Cu_3O_{6.9}$ sample [(a) to (b)] and move the samples [(b) to (c)]. The total energy bandpass (FWHM) is 30 meV. Note how the Fermi energy crosses the middle of the shoulder in both 100-K $YBa_2Cu_3O_{6.9}$ and the 20-K Pt, but almost is on the peak in 20-K $YBa_2Cu_3O_{6.9}$. These spectra were taken with $h\nu=17$ eV and near ($\bar{X}$ and $\bar{Y}$) in the twinned crystal of $YBa_2Cu_3O_{6.9}$ and with a Pt foil. All Fermi energies were $h\nu=17$ eV and near $\bar{X}$ and $\bar{Y}$) in the twinned crystal of $YBa_2Cu_3O_{6.9}$ and with determined from spectra of Pt foil, as illustrated in this figure.

are two overridingly important experimental factors that must be dealt with properly: calibration of the Fermi energy and inclusion of the combined effect of the occupation function and experimental resolution.

The determination of the Fermi energy is fairly straightforward and highly reproducible, as can be gleaned from a consideration of spectrum (c) of Fig. 15. The center or inflection point of the rise is chosen as the Fermi energy. This can be done with a reproducibility of 5 meV. At 20 K the entire Fermi step is only 30 meV wide, from 10% to 90% height positions, which is essentially all due to instrumental broadening. (It can be shown that the 10%–90% width of a step is equivalent to the full width at half maximum of a Gaussian instrument function.) The temperature contribution is 8 meV, a minor effect. The uncertainty in locating the center of this step and the stability of the electronics determine the 5-meV uncertainty. Having dealt with the Fermi-energy calibration and introduced the elements of the resolution of the Fermi occupation function, the $YBa_2Cu_3O_{6.9}$ spectra will be considered in terms of this second factor.

The Fermi occupation function and instrumental broadening can affect the appearance of near-Fermi-edge spectra and limit how well the energy of a nearby peak can be determined. If the temperature is increased, the intrinsic 10%–90% width of a Fermi step function (4.4 kT) increases: At 100 K the temperature contributions would be 37 meV. Not only can the width of the step be affected, but also the shape of a nearby peak. The 10%–90% criteria for determining the resolution is only good if a step function, or step function smeared by a Fermi function, is broadened by a Gaussian instrument function. If there is an additional sharp structure at the edge, the resultant experimental structure will appear to have an edge, as determined by the 10%–90% criteria that is sharper than the instrumental resolution. While this "improvement in resolution" is only the result of the misapplication of the 10%–90% criteria, it is an excellent indicator of the existence of a sharp structure at or near the Fermi level. A second indicator is that, as the structure sharpens, the Fermi level will shift toward the peak. The limiting case of a δ function at the Fermi level is somewhat intuitive: After convolution, the measured shape will be the instrumental function, and the Fermi level will be at the peak. The measured peak position is also distorted. As an example, a Lorentzian centered at the Fermi level will be only half occupied. Applying a Fermi function will result in a peak that is below the Fermi level. Convolution by an instrument function will further broaden the structure and move the resultant peak to even deeper binding energy.

Now let us apply this to a consideration of the $YBa_2Cu_3O_{6.9}$ spectra in Fig. 15. It is reassuring that the Fermi energy, as determined from the Pt foil, falls near the center of the rise in the 100-K spectrum (a). Moreover, the width of the edge also makes sense, in light of the larger temperature contribution to the broadening (37 meV) at 100 K. Applying Fermi statistics to the 100-K sample is reasonable because the 100-K sample is in the normal state. The 20-K spectrum exhibits the effects discussed above. First, the peak is within about 10 meV of the Fermi energy, as determined by the bracketing measurements of (a) and (c). Second, the rise near the Fermi energy is dramatic and even sharper than that of the Pt foil at 20 K, with the initial rise at the same energy as 100-K $YBa_2Cu_3O_{6.9}$ and 20-K Pt. Since the rise is actually sharper than the 20-K Pt Fermi edge, we have a clear indication of a structure that is narrow on the scale of the instrument resolution. This is confirmed by the position of the Fermi level.

Based upon the above arguments and observations, if a gap does exist, it has a width of $\Delta \leq 5\pm5$ meV. The presence of electronic density near the Fermi energy is consistent with several other seemingly anomalous observations of $YBa_2Cu_3O_{6.9}$. For example, tunneling measurements exhibit both a nonzero conductance at zero bias and a linear background conductance in the gap.[30] Specific-heat,[35] Raman-scattering,[36] and microwave-resistivity measurements[37] all suggest electronic density inside the large gap observed by other measurements. Although the rough estimate of the apparent gap width, $\Delta \leq 5\pm5$ meV, applies to all the crossings, both chain- and plane-derived, which we have observed, assignment of the electronic density to specific electronic structure must wait further analysis. In the succeeding paragraphs, possible causes and origins of the apparent small gap will be discussed, including its relationship to the plane- and chain-derived bands.

To begin, consider the apparent discrepancy between the results for cleaved $Bi_2Sr_2CaCu_2O_8$ (Ref. 2) and cleaved $YBa_2Cu_3O_{6.9}$. In retrospect, it really is not

surprising that the results are different. The lattice structure of $Bi_2Sr_2CaCu_2O_8$ has two very noticeable simplifications relative to $YBa_2Cu_3O_{6.9}$: the absence of chains and the presence of mirror plane symmetry *between* the two weakly bonded cleavage layers, so that intact unit cells survive cleavage and thus exist on the surface for photoemission measurements. Such mirror-cleavage planes do not exist in $YBa_2Cu_3O_{6.9}$, and so cleaving implies some sort of asymmetry or a rupturing of the topmost unit cell. We will return to this issue shortly, but first the impact of chains will be discussed.

The chain states may be masking a gap in the plane states.[38] Our best estimate of the apparent gap comes from what are believed to be chain states, and all of our crossings, including those of the plane-derived bands, have nearby chain bands. Perhaps the small gap is a chain property only and the CuO plane gaps are hidden by the chain intensity near the Fermi energy. Consider the spectra of Fig. 11 and Fig. 9(b). The band-2 crossing and gap may be obfuscated by the small chain gap possibly associated with band 1. This picture is appealing in light of the other measurements of gaps, which indicate a large CuO plane gap (for example, Ref. 29) and two gap structures with a smaller gap for the chains.[31,33,34]

Another possibility is the combination of cleavage-induced surface reconstruction and a proximity effect. Perhaps the process of cleaving produces a subtle, but telling shift of atoms. Despite the rupturing of unit cells, it would be necessary that the two-dimensional periodicity remain intact, based upon our observation of such detailed spectral structure around $\bar{\Gamma}$, $\bar{X}$, $\bar{Y}$, and $\bar{S}$. Perhaps a slight vertical expansion or contraction of the lattice is occurring. For example, a reduced volume could give rise to the increased orthorhombicity and decreased critical temperature proposed by Hayashi.[39] If the critical temperature dropped below 20 K, the surface of the material would be normal. (Perhaps then the changes that are seen in Fig. 15 are solely due to thermal broadening.) Alternatively, there is evidence from resistivity measurements that chain imperfections (oxygen depletion) can give rise to a metallic band. Perhaps the cleavage causes oxygen loss in the chain bands. To address the issue of surface obfuscation of bulk gaps, a series of gas-adsorption studies were performed with Ar and O_2. The hypothesis was that Ar or O_2 would change the reconstruction and open up a large gap: This did not occur. However, it is unclear whether gas adsorption is sufficiently severe to perturb a reconstruction that may be one-half of a unit cell deep (~ 6 Å).

Thus, although it is not possible to uniquely assign the origin of the small gap, it seems fairly likely that it is strongly chain related. The observation of the $\bar{Y}$ Fermi-energy peak and the differences with $Bi_2Sr_2CaCu_2O_8$ both point toward strong participation by the chain-derived states.

IV. SUMMARY

High-resolution angle-resolved photoemission studies of untwinned, single-crystal $YBa_2Cu_3O_{6.9}$ have been performed. Remarkably acute spectral structure both at and away from the Fermi energy has been observed. Strong indications of the twofold symmetry have been seen, and Fermi-surface measurements exhibit an almost quantitative agreement with the predictions of LDA calculations. The absence of the observation of a large gap was demonstrated, and the strong connection of the small gap to chain-derived states was discussed.

ACKNOWLEDGMENTS

Work performed under the auspices of the U.S. Department of Energy by Lawrence Livermore National Laboratory under Contract No. W-7405-ENG-48 and Ames Laboratory under Contract No. W-7405-ENG-82. The synchrotron-radiation investigations were performed at the University of Wisconsin Synchrotron Radiation Center. Conversations with Vladimir Kresin were highly enlightening, enjoyable, and appreciated.

[1]R. Manzke, T. Buslaps, R. Cleaesen, and J. Fink, Europhys. Lett. **9**, 477 (1989); T. Takahashi, H. Matsuyama, H. Katayama-Yoshide, Y. Okabe, S. Hosoya, H. Seki, H. Fujimoto, M. Sato, and H. Inokuchi, Nature **334**, 691 (1988); R. Manzke, T. Buslaps, R. Claessen, M. Skibowski, and J. Fink, Physica C **162-164**, 1381 (1989); G. Mante, R. Claessen, T. Buslaps, S. Harm, R. Manzke, M. Skibowski, and J. Fink, Z. Phys. B **80**, 181 (1990).

[2]C. G. Olson, R. Liu, A.-B. Yang, D. W. Lynch, A. J. Arko, R. S. List, B. W. Veal, Y. C. Chang, P. Z. Jiang, and A. P. Paulikas, Science **245**, 731 (1989); C. G. Olson, R. Liu, D. W. Lynch, R. S. List, A. J. Arko, B. W. Veal, Y. C. Chang, P. Z. Jiang, and A. P. Paulikas, Solid State Commun. **76**, 411 (1990); Phys. Rev. B **42**, 381 (1990); C. G. Olson, R. Liu, D. W. Lynch, B. W. Veal, Y. C. Chang, P. Z. Jiang, J. Z. Liu, A. P. Paulikas, A. J. Arko, and R. S. List, Physica C **162-164**, 1697 (1989).

[3]J. C. Campuzano, G. Jennings, M. Faiz, L. Beaulaigue, B. W. Veal, J. Z. Liu, A. P. Paulikas, K. Vandervoort, H. Claus, R. S. List, A. J. Arko, and R. J. Bartlett, Phys. Rev. Lett. **64**, 2308 (1990).

[4]Y. Sakisaka, T. Komeda, T. Maruyama, M. Onchi, H. Kato, Y. Aiura, H. Yanashima, T. Terashima, Y. Bando, K. Iijima, K. Yamamoto, and K. Hirata, Phys. Rev. B **39**, 9086 (1989).

[5]A. J. Arko, R. S. List, R. J. Bartlett, S.-W. Cheong, Z. Fisk, J. D. Thompson, C. G. Olson, A. B. Yang, R. Liu, C. Gu, B. W. Veal, J. Z. Liu, A. P. Paulikas, K. Vandervoort, H. Claus, J. C. Campuzano, J. E. Schirber, and N. D. Shinn, Phys. Rev. B **40**, 2268 (1989).

[6]W. E. Pickett, H. Krakauer, R. E. Cohen, and D. J. Singh, Science **225**, 46 (1992); J. Yu and A. J. Freeman, Bull. Am. Phys. Soc. **36**, 770 (1991).

[7]J. C. Campuzano *et al.* (unpublished); J. C. Campuzano *et al.*, Bull. Am. Phys. Soc. **36**, 1028 (1991).

[8]C. G. Olson, Nucl. Instrum. Methods A **266**, 205 (1988).

[9]J. Z. Liu, M. D. Lan, P. Klavins, and R. N. Shelton, Phys. Lett. A **144**, 265 (1990).

[10]R. Claessen, G. Mante, A. Huss, R. Manske, M. Skibowski,

Th. Wolf, and J. Fink, Phys. Rev. B **44**, 2399 (1991); G. Mante, R. Claessen, A. Huss, R. Manske, M. Skibowski, Th. Wolf, M. Knupfer, and J. Fink, *ibid.* **44**, 9500 (1991).

[11]C. G. Olson *et al.* (unpublished).

[12]S. Massida, J. Yu, A. J. Freeman, and D. D. Koelling, Phys. Lett. A **122**, 198 (1987); J. Yu, S. Massida, A. J. Freeman, and D. D. Koeling, *ibid.* **122**, 203 (1987).

[13]W. E. Pickett, R. E. Cohen, and H. Krakauer, Phys. Rev. B **42**, 8764 (1990).

[14]M. Hirao, T. Uda, and Y. Murayama (unpublished).

[15]B. H. Brandow, J. Solid State Chem. **88**, 28 (1990).

[16]S. John and P. Voruganti, Phys. Rev. B **43**, 10 815 (1991); J. B. Grant and A. K. McMahan, Phys. Rev. Lett. **66**, 488 (1991).

[17]N. V. Smith and P. K. Larsen, in *Photoemission and the Electronic Properties of Surfaces,* edited by B. Feuerbacher, B. Fitton, and R. F. Willis (Wiley-Interscience, New York, 1978).

[18]J. G. Tobin, S. W. Robey, and D. A. Shirley, Phys. Rev. B **33**, 2270 (1986); J. G. Tobin, S. W. Robey, L. E. Klebanoff, and D. A. Shirley, *ibid.* **35**, 9056 (1987).

[19]M. S. Islam and R. C. Baetzold, Phys. Rev. B **40**, 10 926 (1989); M. A. Beno, L. Soderholm, D. W. Capone II, D. G. Hinks, J. D. Jorgensen, I. K. Schuller, C. U. Segre, K. Zhang, and J. D. Grace, Appl. Phys. Lett. (to be published).

[20]A. Kotani and Y. Toyozawa, in *Synchrotron Radiation Techniques and Applications,* edited by C. Kunz (Springer-Verlag, Berlin, 1979).

[21]S. Nakai, N. Nücker, H. Romberg, M. Alexander, and J. Fink, Phys. Scr. **41**, 596 (1990).

[22]R. H. Victora and L. M. Falicov, Phys. Rev. Lett. **55**, 1140 (1985); A. Liebsch, Phys. Rev. B **23**, 5203 (1981); O. Gunnarson and K. Schönhammer, *ibid.* **22**, 3710 (1980).

[23]S. G. Louie, P. Thiry, R. Pinchaux, Y. Petroff, D. Chanderis, and J. Lecante, Phys. Rev. Lett. **44**, 549 (1980); S. D. Kevan, N. G. Stofrel, and N. V. Smith, Phys. Rev. B **31**, 3348 (1985).

[24]For example, see J. G. Nelson, S. Kim, W. J. Gignac, R. S. Williams, J. G. Tobin, S. W. Robey, and D. A. Shirley, Phys. Rev. B **32**, 3465 (1985), and references therein.

[25]J. L. Smith, C. M. Fowler, B. L. Freeman, W. L. Hults, J. C. King, and F. M. Mueller, Bull. Am. Phys. Soc. **36**, 515 (1991).

[26]G. Kido, K. Komorita, H. Katayama-Yoshida, T. Takahashi, Y. Kitaoka, K. Ishida, and T. Yoshitomi, Bull. Am. Phys. Soc. **36**, 515 (1991).

[27]H. Haghighi, J. H. Kaiser, S. Rayner, R. N. West, J. Z. Liu, R. Shelton, R. Howell, F. Solal, and M. J. Fluss, Phys. Rev. Lett. **67**, 382 (1991).

[28]R. Liu, B. W. Veal, A. P. Paulikas, J. W. Downey, H. Shi, C. G. Olson, C. Gu, A. J. Arko, and J. J. Joyce, Phys. Rev. B **45**, 5614 (1992).

[29]R. T. Collins, Z. Schlesinger, F. Holtzberg, and C. Field, Phys. Rev. Lett. **63**, 422 (1989); D. Van der Marel, M. Bauer, E. H. Brandt, H. U. Habermeier, D. Heitmann, W. Konig, and A. Wittlin, Phys. Rev. B **43**, 8606 (1991).

[30]M. Gurvich, J. M. Valles, Jr., A. M. Cucold, R. C. Dynes, J. P. Gamo, L. F. Schneemeyer, and J. V. Waszczak, Phys. Rev. Lett. **63**, 1008 (1989).

[31]V. Z. Kresin and S. A. Wolf, Physica C **169**, 476 (1990).

[32]S. E. Barrett, D. J. Durand, C. H. Pennington, C. P. Slichter, T. A. Friedmann, J. P. Rice, and D. M. Ginsberg, Phys. Rev. B **41**, 6283 (1990).

[33]E. T. Heyen, M. Cardona, J. Karpinski, E. Kaldis, and S. Rusieki, Phys. Rev. B. **43**, 12 958 (1991).

[34]K. F. McCarty, J. Z. Liu, R. N. Shelton, and H. R. Radousky, Phys. Rev. B **42**, 9973 (1990); K. F. McCarty, H. B. Radousky, J. Z. Liu, and R. N. Shelton, *ibid.* **43**, 13 751 (1991).

[35]S. Vonmolnar, A. Torressen, D. Kaiser, F. Holtzberg, and T. Penney, Phys. Rev. B **37**, 3762 (1988).

[36]S. L. Cooper, M. V. Klein, B. G. Pazol, J. P. Rice, and D. M. Ginsberg, Phys. Rev. B **37**, 5920 (1988).

[37]V. F. Gantmakher, V. I. Kulakov, G. I. Leview, R. K. Nikolaev, A. V. Polisskii, N. Sidorov, and M. R. Trunin, Physica C **162**, 1539 (1989); J. P. Ganne, R. Kormann, M. Labeyrie, F. Lainee, and B. Lloret, *ibid.* **162**, 1541 (1989).

[38]V. Z. Kresin, S. A. Wolf, and G. Deutscher (unpublished); V. Z. Kresin and S. A. Wolf, Phys. Rev. B **41**, 4278 (1990).

[39]H. Hayashi (unpublished).